Structural and Functional Modeling of Human Lysozyme Reveals a Unique Nonapeptide, HL9, with Anti-HIV Activity †

ARTICLE *in* BIOCHEMISTRY · MARCH 2005

Impact Factor: 3.02 · DOI: 10.1021/bi0477081 · Source: PubMed

9 AUTHORS, INCLUDING:

Sylvia Lee-Huang
New York University
75 PUBLICATIONS **2,483** CITATIONS
SEE PROFILE

Paul Huang
Massachusetts General Hospital
214 PUBLICATIONS **21,280** CITATIONS
SEE PROFILE

Structural and Functional Modeling of Human Lysozyme Reveals a Unique Nonapeptide, HL9, with Anti-HIV Activity†

Sylvia Lee-Huang,*,‡ Vladimir Maiorov,§ Philip L. Huang,‡ Angela Ng, Hee Chul Lee, Young-Tae Chang, Neville Kallenbach, Paul L. Huang,‡ and Hao-Chia Chen*

Department of Biochemistry, New York University School of Medicine, New York, New York 10016, American Biosciences, Boston, Massachusetts 02114, Department of Chemistry, New York University, New York, New York 10003, Department of Medicine, Massachusetts General Hospital and Harvard Medical School, Boston, Massachusetts 02114, and Endocrinology and Reproduction Research Branch, National Institute of Child Health and Human Development, NIH, Bethesda, Maryland 20892

Received October 27, 2004; Revised Manuscript Received December 13, 2004

ABSTRACT: We previously reported that lysozyme accounts for anti-HIV activity associated with the β-core fraction of human chorionic gonadotropin [Lee-Huang, S., Huang, P. L., Sun, Y., Kung, H. F., Blithe, D. L. & Chen, H. C. (1999) *Proc Natl Acad Sci U S A 96*, 2678−81]. To define the structural and sequence requirements for anti-HIV activity, we carried out peptide fragmentation and activity mapping of human lysozyme. We identified two peptides that consist of 18 and 9 amino acids of human lysozyme (HL18 and HL9), corresponding to residues 98−115 and 107−115. HL18 and HL9 are potent inhibitors of HIV-1 infection and replication with EC_{50}s of 50 to 55 nM, comparable to intact lysozyme. Scrambling the sequence or substitution of key arginine or tryptophan residues results in loss of antiviral activity. HL9, with the sequence RAWVAWRNR, is the smallest peptide we identified with full anti-HIV activity. It forms a pocket with its basic residues on the surface of the molecule. HL9 exists as an α-helix in native human lysozyme, in a region of the protein distinct from the muramidase catalytic site. Monte Carlo peptide folding energy minimizing simulation modeling and CD studies indicate that helical propensity does not correlate with antiviral activity. HL9 blocks HIV-1 viral entrance and replication, and modulates gene expression of HIV-infected cells, affecting pathways involved in survival, stress, TGFβ, p53, NFκB, protein kinase C and hedgehog signaling.

Lysozyme, discovered by Sir Alexander Fleming in 1922 (*1*), is an important innate host defense protein. Lysozyme is a muramidase, which hydrolyzes the β 1−4 glycosidic linkage between *N*-acetylmuramate and *N*-acetylglycosamine in the cell wall of Gram-positive bacteria. In addition, lysozyme has antitumor and antiviral activities, and enhances the immune system (*2*−*7*). In 1999, we discovered that human lysozyme is a highly active anti-HIV component associated with the β-core fraction of human chorionic gonadotropin from urine of pregnant women (*8*).

To define the molecular mechanism of human lysozyme's anti-HIV activity, we carried out structure/activity mapping and molecular modeling. Specifically, we asked whether muramidase activity is critical to anti-HIV activity, and whether different domains or catalytic sites are involved in these processes. We report here that the anti-HIV activity of lysozyme is independent of its muramidase activity. We discovered two peptides, HL18 and HL9, which are as active as lysozyme itself. HL9 is the smallest fragment of human lysozyme with full anti-HIV activity. Amino acid substitution experiments reveal the importance of individual arginine and tryptophan residues to anti-HIV activity.

Both HL18 and HL9 are located within the helix-loop-helix (HLH) motif closest to the C-terminus of lysozyme. Peptide folding modeling and CD spectroscopy studies show that HL9 can adopt α-helical structure in a helicogenic solvent. However, helical propensities do not correlate with antiviral activity. We defined the biological activity of HL9, and show that it blocks HIV-1 viral infection and replication. HL9 also affects the host cell expression of genes involved in specific signaling pathways.

Lysozyme appears to be part of an innate immune system designed to eliminate a broad spectrum of intruders. It is an important first line of defense that can respond well before the adaptive immune system is mobilized. As we identify new functions for this venerable molecule, we hope to define new approaches in therapeutics by utilizing and enhancing our own natural defenses against pathogens.

EXPERIMENTAL PROCEDURES

Proteolytic Fragmentation. Proteolytic fragmentation of human lysozyme was carried out with clostripain, which cleaves at the C-terminal side of arginine residues. Clostripain (Sigma) was dissolved in 50 mM Tris buffer pH 7.6 containing 10 mM $CaCl_2$, 150 mM NaCl, and 2 mM DTT at 200U/ml, and activated at room temperature for 2 h before use. Human lysozyme was dissolved in Tris buffer, pH 7.6 at 2−10 mg/mL. Proteolytic fragmentation was carried out

* Corresponding Authors.
† Supported by PHS grant R01-AT01383 to SLH.
‡ Dedication: This paper is dedicated to the memory of Mrs. An Fu Lee, devoted and beloved mother and grandmother.
§ Current address: Merck Research Laboratories, Rahway, NJ.

10.1021/bi0477081 CCC: $30.25
Published on Web 03/05/2005

using activated clostripain (10 U/mg lysozyme) at 37 °C for 18 h.

Analysis of Proteolytic Fragments. The clostripain digest was centrifuged at 15,000 g for 20 min, and the supernatant was resolved by reversed phase chromatography on a ProRPC Hr 16/10 column (Pharmacia) equilibrated with 0.3% (v/v) TFA. The column was eluted with a linear gradient of acetonitrile from 0 to 60% (v/v). Fractions were assayed for anti-HIV activity by effects on p24 production in HIV-1 infected H9 lymphocytes. Peak fractions were pooled and rechromatographed through a ProRPC Hr5/5 column with a linear gradient of acetonitrile from 0 to 60% (v/v).

Peptides. The peptides HL9 and HL18, as well as mutant peptides carrying amino acid substitutions, were synthesized by GeneMed Synthesis, Inc (South San Francisco, CA) using Fmoc (9-fluorenylmethyloxycarbonyl) methodology. The peptides were purified by HPLC using reverse phase C18 column chromatography. The purity of the final products is >95% by analytical RP-HPLC and MALDI-mass spectrometry.

Cell Lines and Viruses. The MT2 cell line was used as indicator cell for the microtiter syncytium formation assay. The H9 cell line was used for p24 expression assay. Cells were cultured in RPMI medium 1640 containing 100 U/ml penicillin, 100 μg/mL streptomycin, 2 mM L-glutamine, and 10% heat-inactivated fetal calf serum. HIV-1IIIB virus was prepared and stocked as described previously (*8*). Cell lines and virus stock were obtained through the AIDS Research and Reference Reagent Program, Division of AIDS, NIAID, NIH.

Anti-HIV and Cytotoxicity Assays. The effects of HL18 and HL9 on acute HIV infectivity were measured by the microtiter syncytium formation assay (*9*). Briefly, HIV-1 infectivity is determined by measuring syncytium formation in the infectious cell center assay by co-culturing HIV-infected H9 cells (H9−HIV-1) and uninfected MT2 target cells. Effects on viral replication were measured by HIV-1 core protein p24 expression by ELISA at days 4 and 5. EC_{50} in these assays is defined as the concentration at 50% inhibition (*10*). Cytotoxicity of HL18 and HL9 was evaluated by the MTT assay at days 2 to 6 (*11*).

cDNA Microarray Analysis. Profiling of HIV-1 infection and the effects of HL9 and HL18 on target cell gene expression were performed by cDNA microarray analysis (*12*). Pathway specific arrays were obtained from Super Array Inc. (Bethesda, MD). Five μg of total RNA was used as template for ^{32}P cDNA probe synthesis using a mixture of pathway specific primers. The cDNA probe was hybridized to the cDNA array, washed at a stringency of 0.1× SSC, 0.5% SDS at 60 °C six times, and exposed to film. Each array is composed of 96 marker genes in tetra-spot format. The intensity of the signals was quantitated using NIH Image software.

Lysozyme Assay. Lysozyme activity was determined by the turbidimetric assay (*13*), using 0.015% (w/v) cell suspension of Micrococcus lysodeikticus (ATCC 4698) as the substrate. Decrease in turbidity due to lysozyme-catalyzed cell lysis was measured at 450 nm.

Structural Analysis and Modeling. Human lysozyme 3D structure was taken from Protein Data Bank (PDB code 1LZS). Protein structure analysis, visualization and peptide modeling were done using program ICM (*14*, *15*). Secondary structure of the modeled peptide conformations was determined according to method DSSP (*16*) as implemented in ICM.

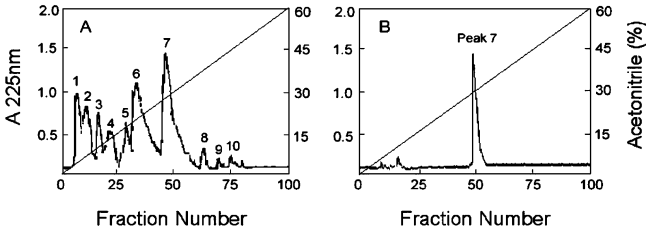

FIGURE 1: Identification and purification of fragments with anti-HIV activity from clostripain digestion of human lysozyme. (A) Elution profile of human lysozyme clostripain digest from reversed-phase chromatography on a ProRPC Hr 16/10 column. Peak 7 contained anti-HIV activity. (B) Purification of peak 7 by reversed-phase chromatography on a ProRPC (Hr5/5) column.

Circular Dichroism Measurements. CD spectra were recorded on an AVIV 62-DS CD spectrometer, using 1 mm sample cells and a fixed temperature of 4 °C. Each spectrum is a smoothed average of 10 scans. The bandwidth for each measurement was 1 nm. The CD spectra of the peptides were measured in 50 mM sodium phosphate buffer pH 7.4 (SP) and in SP containing 40% trifluoroethanol (TFE/SP). CD intensities are expressed as mean residue ellipticities (degrees cm^2 /dmol). Prior to calculation of the final ellipticity, all spectra were corrected by subtracting the reference spectra of TFE/SP without peptides.

RESULTS

Identification and Purification of a Fragment of Human Lysozyme with Anti-HIV Activity. We carried out limited proteolytic fragmentation of human lysozyme with clostripain, and resolved the digest by reversed phase chromatography into 10 peptide peaks (Figure 1A). The bulk of anti-HIV activity was found in peak 7. Pooled peak 7 fractions were repurified by reversed phase chromatography (Figure 1B). We confirmed anti-HIV activity of this material, and characterized the purified peptide by amino acid sequencing.

Edman degradation sequence analysis revealed that the peptide in peak 7 consists of 18 amino acids with the sequence RVVRDPQGIRAWVAWRNR. This corresponds to residues 98−115 of human lysozyme (*17*), so it was designated HL18. Table 1 summarizes the anti-HIV properties of HL18. It inhibits both viral infection and replication, as assayed by HIV syncytium formation and core antigen p24 expression. The EC_{50} values for HL18 are 58 nM for syncytium formation and 62 nM for core antigen p24 expression, as compared with EC_{50}s for intact human lysozyme of 55 and 64 nM. Chemically synthesized HL18 and HL18 purified from clostripain digestion displayed similar anti-HIV activity.

Structure−Function Analysis of Human Lysozyme Fragments. To gain insight into the role of specific amino acids in the anti-HIV activity of HL18, we performed a series of amino acid replacement experiments (Table 1). Substitution of tryptophan (W) 109 or 112 by tyrosine (Y) results in complete loss of anti-HIV activity. Substitution of the positively charged arginine (R) at positions 98 or 101 with lysine (K) or asparagine (N) does not significantly affect anti-HIV activity. Substitution of arginine (R) with asparagine

Table 1: Mapping of Anti-HIV Activity in Peptides from Human Lysozyme

Peptide	Sequence	Anti-HIV EC_{50} (syncytia)	Anti-HIV EC_{50} (p24)
Lysozyme	Whole molecule	55 nM	64 nM
HL18 (peak 7)	RVVRDPQGIRAWVAWRNR	58 nM	62 nM
HL18 (synthetic)	RVVRDPQGIRAWVAWRNR	54 nM	66 nM
HL18 (W109→Y)	RVVRDPQGIRAYVAWRNR	No activity	No activity
HL18 (W112→Y)	RVVRDPQGIRAWVAYRNR	No activity	No activity
HL18 (R98→K)	KVVRDPQGIRAWVAWRNR	60 nM	68 nM
HL18 (R101→N)	RVVNDPQGINAWVAWRNR	60 nM	66 nM
HL18 (R107→N)	RVVRDPQGINAWVAWRNR	>100 μM	>100 μM
HL18 (R113→K)	RVVRDPQGIRAWVAWKNR	>100 μM	>100 μM
HL18 (R115→K)	RVVRDPQGIRAWVAWRNK	>100 μM	>100 μM
HL18 N-terminus	RVVRDPQGI	No activity	No activity
HL9	RAWVAWRNR	50 nM	55 nM
HL9 scrambled	AWRWRARVN	No activity	No activity
HL9 (W109→Y)	RAYVAWRNR	No activity	No activity
HL9 (W112→Y)	RAWVAYRNR	No activity	No activity
HL9 (R107→N)	NAWVAWRNR	>100 μM	>100 μM
HL9 (R113→K)	RAWVAWKNR	>100 μM	>100 μM
HL9 (R115→K)	RAWVAWRNK	>100 μM	>100 μM
HL9 (107-111)	RAWVA	No activity	No activity
HL9 (109-113)	WVAWR	No activity	No activity
HL9 (111-115)	AWRNR	No activity	No activity

(N) at positions 107, or with lysine (K) at positions 113, or 115 reduces antiviral activity.

We noted that substitutions that affect anti-HIV activity are all located in the C-terminal half of HL18. Both the hydrophobic amino acid tryptophan and the positively charged arginine residues in the C-terminal half of HL18 are critical for the anti-HIV activity. In view of these results, we synthesized two 9 amino acid peptides corresponding to the N- and C-terminal halves of HL18. The N-terminal nonapeptide of HL18 has no anti-HIV activity, while the C-terminal nonapeptide of HL18 has full anti-HIV activity. We named this C-terminal 9 amino acid peptide HL9, and carried out further structure−function analysis.

Peptides with the same amino acid composition as HL9, but with scrambled sequence, possess no measurable anti-HIV activity. Amino acid substitution experiments varying charge and hydrophobicity resulted in analogous results for HL9 as obtained for HL18 (Table 1). To test whether smaller peptide fragments of human lysozyme possess anti-HIV activity, we synthesized three overlapping pentapeptides corresponding to amino acids 107−111, 109−113, and 111−115. No anti-HIV activity is found in any of these peptides. Thus, HL9 is the smallest fragment of human lysozyme we identified with full anti-HIV activity.

Biological Effects of Lysozyme, HL9, and Inactive Mutants. We characterized the effects of HL9 on acute HIV-1 infection and cell-to-cell transmission. Early events in acute viral infection, including viral fusion and entry, are reflected in the syncytium formation assay. Effects on HIV-1 replication are reflected in viral core antigen p24 expression. Figure 2 shows the concentration dependence of the effects of lysozyme, HL9, and an inactive mutant W109Y on HIV cell-to-cell transmission and acute infection as measured by syncytium formation (Figure 2A) and core protein p24 production (Figure 2B). The EC_{50}s of HL9 for inhibition of syncytia formation and p24 production are 50nM and 55nM. The EC_{50}s for lysozyme in these assays are 55 nM and 64 nM. In contrast, the HL9 mutant W109Y showed no activity over the entire concentration range of the assay. Figure 2C shows the effect of HL9 on the viability of the target cells as measured by the MTT assay. No cytotoxicity was detected over the effective dose range of the anti-HIV assay, over a 10,000-fold concentration range from 1 nM to 100 μM. Cell viability, as determined by trypan blue dye exclusion, was

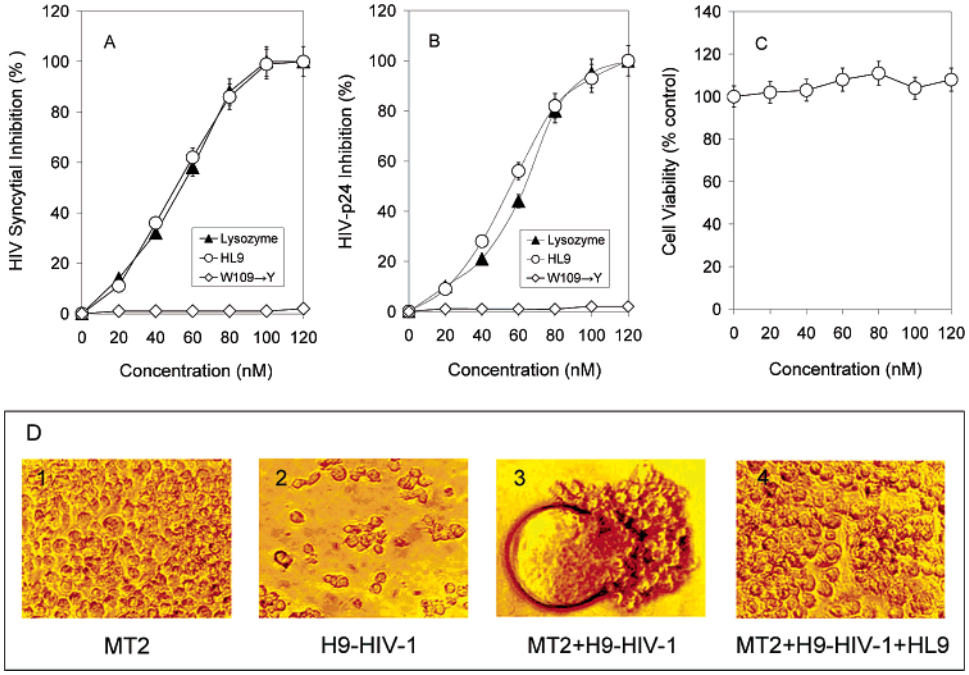

FIGURE 2: Anti-HIV activities of lysozyme, HL9, and HL9 mutant W109Y. (A) Concentration dependence of the effects of lysozyme, HL9, and HL9 mutant W109Y on syncytia formation in HIV-infected MT2 cells. (B) Concentration dependence of the effects of lysozyme, HL9, and HL9 mutant W109Y on HIV core protein p24 expression in HIV-infected H9 cells. (C) Cytotoxicity of HL9 assayed by the MTT assay with target H9 and MT2 cells. (D) Effects of HL9 on syncytia formation. (1) Uninfected MT2 target cells. (2) HIV-infected H9 cells. (3) Co-culture of MT2 target cells with HIV-infected H9 cells, resulting in the formation of multinucleated giant cells (syncytia). (4) HL9 treated co-cultures, showing no syncytia formation.

also unaffected by HL9. Figure 2D illustrates that HL9 treatment prevents syncytia formation in co-cultures of HIV-infected H9 cells and MT2 target cells. While HL18 and HL9 are as potent as intact human lysozyme against HIV-1, they exhibit no muramidase activity.

Sequence Homology Analysis of HL9. We searched the SWISSPROT database with more than 79,000 sequences by the BLAST program. Only mammalian lysozyme entries LYC-TRIVU, GORGO, HUMAN, HYLLA, PONPY were obtained among the top scoring hits when the original 9 residue sequence of HL9 (RAWVAWRNR) was posed as a query. Additional database searches were carried out with the alternative 9-residue sequence variants [RK] [AVFIL] [WSTY] [AVFIL] [AVFIL] [WSTY] [RK] [NQ] [RK], and the same mammalian lysozyme sequences were found. Two additional sequence databases were searched with HL9 sequence query using the BLAST program: the NCBI non-redundant (NR) database, with about 1,800,000 sequences, and the Database of Antimicrobial Peptides, ANTIMIC (http://research.i2r.a-star.edu.sg/Templar/DB/ANTIMIC), with about 1,700 sequences. The "expect" threshold parameter was set to 20000 for the NR database and to 1000 for the ANTIMIC database to ensure that all significant hits would be found; other BLAST search parameters were used at their default values. For the NR list of hits, the first lysozyme-unrelated hit appeared at an E-value of 5.3, and for the ANTIMIC hit list, it appeared at an E-value of 8.9. These results indicate that the sequence of HL9 is unique, despite its short length.

Three-Dimensional Structure of HL18 and HL9 in Human Lysozyme: the Anti-HIV Site is Distinct from the Hydrolytic Site. Figure 3A shows a ribbon representation of the 3D structure of human lysozyme (*18*). HL18 begins at R98 and continues through the β-turn loop with residues 100−106, to helix 4 (H4) with residues 107−115. HL9, which corresponds to residues 107−115, comprises the entire helix 4, and is located near the C-terminus. Figure 3B shows a peptide folding model of HL9. The anti-HIV site is distinct from the muramidase active site. Figure 3C represents superposition of HL9 onto the corresponding part of the PDB structure of lysozyme. Figure 3D depicts the electrostatic potential distribution on the surface of human lysozyme with two substrate saccharide fragments, $(NAG)_4$ and $(NAG)_2$, bound to the muramidase catalytic site (*19*). Acidic residues, including the active site residues E35 and D52, contribute to a region of negative charges (shown in red) at the muramidase site. In contrast, the basic amino acids R107, R113, R115 and N114 in HL9, critical to anti-HIV activity, form a region of positive charges (shown in blue) on the surface of the molecule. The two sites are distinct in their positions, conformations, charge distributions and local environments. The locations of HL9 and HL18 on the linear amino acid sequence of lysozyme are shown in Figure 3E.

Helical Propensity Does Not Correlate with Anti-HIV Activity. We carried out peptide folding modeling (*14*) of native HL9, as well as of the inactive mutants W109Y, W112Y, R113K, R113N, R115K, R115N and the inactive HL9 scrambled sequence AWRWRARVN. Each peptide structure was created from its sequence in fully extended conformation. 100,000 Monte Carlo minimization steps of probability biased MC procedure were applied to generate conformational stacks with the maximal number of conformations equal to 100. After completion of each run, all generated conformations were analyzed for the presence of the secondary structure elements. The helical propensity index was defined as the average number of occurrences of the helical state for the given residues for all the conformations collected in the stack. As seen in Figure 4, the helical

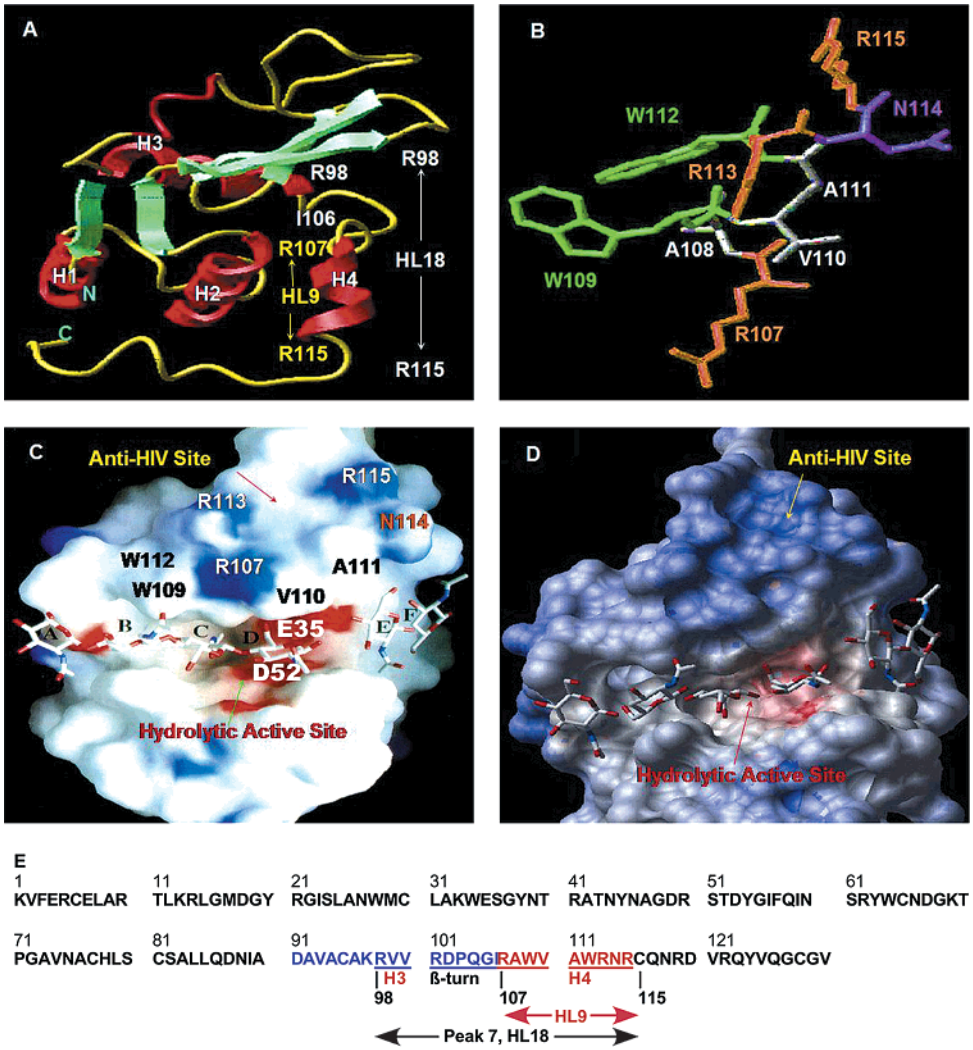

FIGURE 3: Structure and sequence of anti-HIV peptides HL18 and HL9. (A) Ribbon representation of human lysozyme showing the location of HL18 and HL9 fragments. The locations of helices 1−4 (H1−H4) are shown. (B) HL9 conformation determined by peptide folding calculations. Arginines (R) are shown in orange, tryptophans (W) in green, asparagine (N) in purple, and alanine (A) and valine (V) in gray. (C) Superposition of HL9 onto the structure of native lysozyme (1lzs). (D) Distribution of electrostatic potentials on the surface of human lysozyme. A pocket of acidic amino acids contributes to a region of negative charges (red) at the hydrolytic active site. The anti-HIV site (HL9) is located on the surface, surrounded by positively charged R and lined with the hydrophobic W. The basic amino acids R107, 113, 115 and N114 form a region of positive charges (blue). (E) Locations of HL18 and HL9 on the primary amino acid sequence of human lysozyme.

propensity profile for HL9 is below that for the inactive HL9 scrambled peptide, or those of the inactive mutants W109Y and W112Y. The same is true for the other inactive mutants R113K, R113N, R115K, R115N tested (data not shown). Thus, helical conformation does not correlate with anti-HIV activity.

Conformation Preferences of HL9 by Circular Dichroism (CD). To investigate the conformation preferences in relation to anti-HIV activity, we carried out CD spectroscopic analyses of native HL9, the inactive HL9 scrambled sequence, and inactive mutants W109Y and W112Y in different solvent environments. The results are summarized in Figures 4C to 4F. As seen in Figure 4C, in SP, the CD spectrum of HL9 showed a strong negative trough centered below 200 nm, indicating a predominantly random-coil conformation. However, in a solvent system TFE/SP, the CD spectra showed a positive band at 190 nm and double minima at 203 and 220 nm, indicating a highly α-helical conformation (*20*). These results indicate that the HL9 peptide has no inherent propensity for an ordered structure in aqueous solution, but it can adopt a helical conformation in a hydrophobic environment such as TFE/SP (*21*).

The CD spectra of the inactive HL9 scrambled sequence AWRWRARVN and the inactive mutants W109Y and W112Y are shown in Figures 4D, 4E and 4F. All of these inactive peptide derivatives of HL9 showed random-coil conformation in aqueous buffer with negative troughs centered below 200 nm and α-helical conformations in TFE/SP with characteristic positive bands at 190−193 nm and double minima at 203 and 220 nm. These results indicate that in HL9, helicity alone is not sufficient for anti-HIV activity. A positive band at around 230 nm is identified in all of the samples. This is characteristic of the CD spectra of the amino acid tryptophan in unfolded peptides.

Cellular Targets of HL9. To probe cellular targets associated with HIV-1 infection and treatment with HL9 and HL18, we carried out cDNA microarray analyses focused on 18 signal transduction pathways and 96 marker genes. Cellular genes involved in survival, stress, TGFβ, p53, NFκB, protein kinase C and hedgehog signaling pathways are modulated

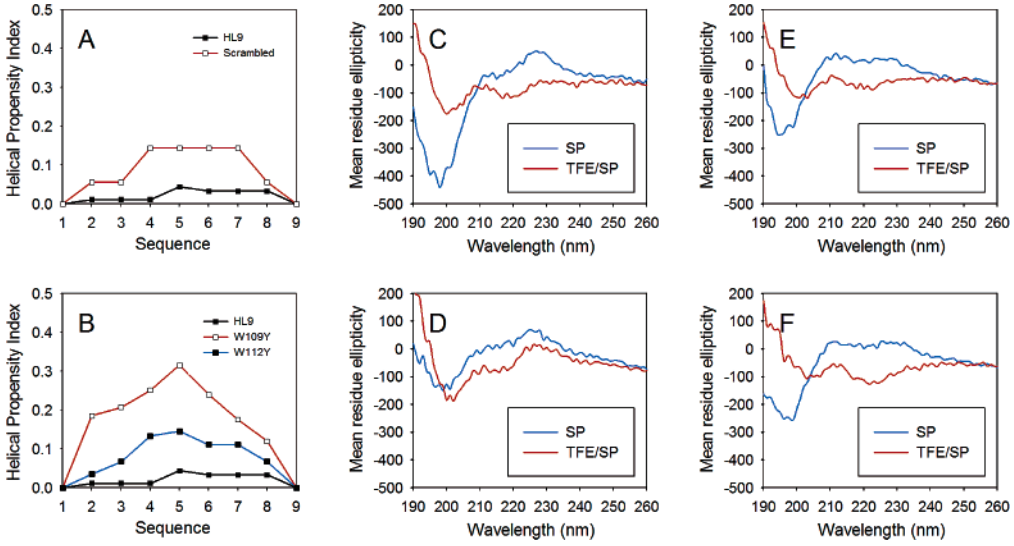

FIGURE 4: Secondary structure of HL9 as determined by peptide folding calculations and conformation preferences of HL9 by circular dichroism (CD). (A) Helical propensity profile of native HL9 RAWVAWRNR (black line) and HL9 scrambled HL9 sequence AWRWRARVN (red line). (B) Helical propensity profile of native HL9 (black line) and the inactive variants W109Y (red line) and W112Y (blue line). (C)−(F) CD spectra showing conformational preferences of the native HL9 sequence, scrambled HL9 sequence, and HL9 inactive variants W109Y and W112Y respectively in aqueous buffer SP (blue lines) or in a hydrophobic environment TFE/SP (red lines).

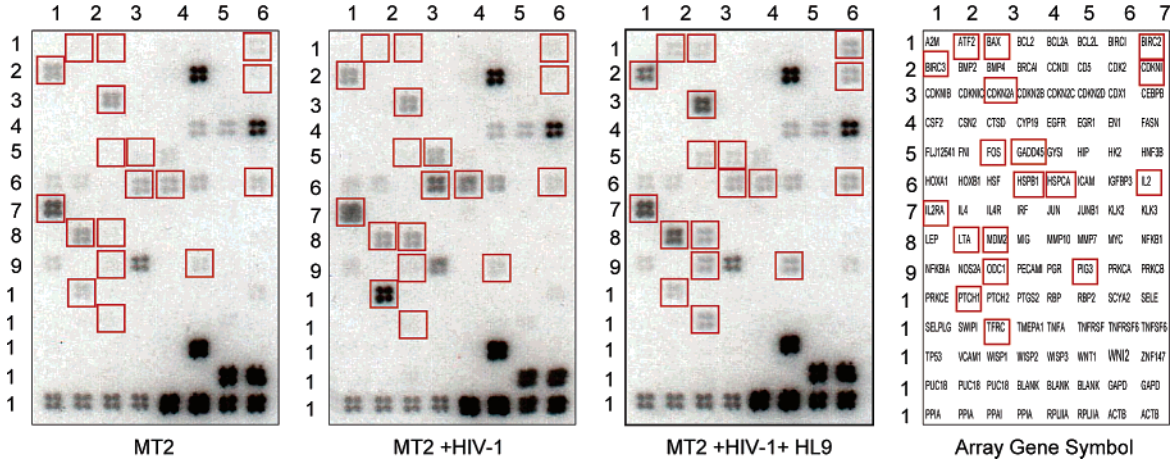

FIGURE 5: Modulation of expression profiles of cellular genes by HIV infection and HL9 treatment. Cellular gene expression profile probed by signal transduction pathway cDNA microarrays. Each array is composed of 96 marker genes in tetra-spot format. Four housekeeping genes are included as positive controls: GAPDH (glyceraldehyde-3-phosphate dehydrogenase), PPIA (peptidylprolyl isomerase A), RPL13A (ribosomal protein L13a) and ACTB (β-actin). The pUC 18 plasmid is included as a negative control. (A) MT2 target cell. (B) HIV-infected MT2. (C) HL9 treated HIV infected MT2. (D) Array layout and gene symbol reference for ease of identification.

in HIV-infection and by HL9 (Figure 5 and Table 2). These include the inhibitor of apoptosis proteins IAP2 (BIRC2) and IAP1 (BIRC3) in the survival pathway; activating transcription factor 2 (ATF2), osteosarcoma viral oncogene homologue (FOS), heat shock proteins hsp27 (HSPB1) and hsp90 (HSPCA) in the stress pathway; cyclin dependent protein kinase inhibitor CDKNIA (p21/waf1/Cip1), and CDKN2A (p16 INK4) in the TGFβ pathway; the BCL2-associated X protein Bax, DNA-damage-inducible transcript gadd45, tumor protein p53 inducible protein 3 (PIG3) and p53 binding protein mdm2 in the p53 and apoptosis pathways; IL-2, IL2RA, p90/Transferrin Receptor (TFRC) and ornithine decarboxylase (ODC1) in the calcium and protein kinase C pathways, and the patched protein (PTCH1) in the hedgehog pathway. HIV-1 infection up-regulates the expression of hsp27, hsp90, gadd45, mdm2 and patched 1 genes while it down-regulates Bax, p21 CIP, and IL-2. Treatment with HL9 or HL18 reverses these HIV-1 infection-associated changes. Treatment of HIV-1 infected cells with HL9 or HL18 also up-regulates the expression of ATF2, Bax, BIRC2, BIRC3, CDKNIA, CDKN2A, FOS, IL-2, IL-2Rα, LTA, ODC1, PIG3 and TFRC genes. No significant changes were noted in the expression of the housekeeping genes GAPDH, PPIA, RPL13A and β-actin.

DISCUSSION

Lysozyme was originally described for its effects against Gram-positive bacteria. This bactericidal property is due to its muramidase activity, which hydrolyzes the peptidoglycan of bacterial cell walls, resulting in cell lysis (*1*). However, an increasing body of evidence suggests the existence of nonenzymic and/or nonlytic modes of action against other microbes. Reduced and/or partially unfolded lysozyme still exerts broad spectrum antimicrobial action against both Gram-negative and Gram-positive bacteria, independent of muramidase catalytic activity (*22*). Moreover, lysozyme is

Table 2: Expression Profile of Signal Transduction-related Genes and Modulation by HIV-1 Infection and HL9 Treatment

UniGene	Genebank	Gene Symbol/Name	MT2	MT2+ HIV	MT2 + HIV + HL9
HS.80258	NM001880	ATF2/Creb-2	VL	VL	↑
HS.159428	NM004324	BAX	VL	VL	↑
HS289107	NM001166	BIRC2/IAP2	VL	VL	↑↑
HS.127799	NM001165	BIRC3/IAP1	M	M	↑↑
HS179665	NM000389	CDKNIA/P21, CIP1	VL	↓	↑↑
HS421319	NM000077	CDKN2A/p16 INK4	M	M	↑↑
HS25647	NM005252	FOS	VL	VL	↑
HS.80409	NM001924	GADD45	VL	↑↑	↓
HS.76067	NM001540	HSPB1/HSP27	L	↑↑↑	↓↓↓
HS.289088	NM005348	HSPCA/HSP90	L	↑↑↑	↓↓↓
HS.89679	NM000588	IL-2	L	↓	↑
HS.130058	NM00417	IL2RA/IL-2 Rα	H	H	↑↑
HS36	NM000595	LTA/TNFβ/LT	L	L	↑↑
HS.170027	NM002392	MDM2 /mdm2	VL	↑	↓
HS.443409	NM002539	ODC1	VL	VL	↑↑
HS50649	NM004881	TP5315/PIG3	VL	VL	↑
HS.159526	NM000264	PTCH1	L	↑↑↑↑	↓↓↓↓
HS185726	NM003234	TFRC/p90/CD71	VL	VL	↑

VL: Very Low Expression, L: Low Expression, M: Moderate Expression, H: High Expression, ↑: Up-regulation, and ↓: Down-regulation. The magnitude of the changes is indicated by the number of arrows: 1 arrow: <2-fold change, 2 arrows: 2 to 5-fold change, 3 arrows: 5 to 10-fold change, 4 arrows: >10-fold change.

widespread in nature and plays critical roles in host defense, both in the control of microbial infection and in the modulation of host immunity (*7*, *23*−*25*).

We previously reported that lysozyme accounts for the anti-HIV activity associated with the β-core fraction of human chorionic gonadotropin (*8*). To better understand the molecular mechanisms of its anti-HIV activity, we carried out peptide fragmentation and activity mapping. We identified two fragments of human lysozyme, HL18 and HL9, which possess full anti-HIV activity comparable to the intact molecule. Anti-HIV activity is sequence-specific, as scrambling the sequence abolishes the activity. Anti-HIV activity is also dependent on charge and hydrophobicity, as substitution of positively charged arginine residues 107, 113, 115 or hydrophobic tryptophan residues 109, 112 result in the loss of anti-HIV activity.

As shown in Figure 3A, the first two amino acids of HL18 belong to the end of helix 3. The next amino acids, VRDPQGI (residues 100−106), constitute the β-turn loop. HL9, RAWVAWRNR (residues 107−115), makes up helix 4. The sequence of HL9 is unique and is found only in mammalian lysozymes. In native lysozyme, HL9 exists as an α-helix, in a region of the protein distinct from the muramidase catalytic site. Thus, muramidase activity and antiviral activity are distinct features of intact human lysozyme, and it is not surprising that HL9 does not display muraminidase activity.

Lysozyme is known to exist in a diverse folding conformations around its active site with different glycan substrates (*18*). A helix-loop-helix motif in hen egg white lysozyme and human lysozyme has been reported to confer antimicrobial activity with membrane permeabilization action (*26*). Energy minimizing simulation predicts that HL9 can adopt α-helical conformation without any flanking sequences essentially identical to that found in the native molecule. CD studies show that HL9 adopts α-helical conformations mainly in a solutions containing TFE, while it assumes a random-coil structure in aqueous buffer. Modeling and CD studies indicate that helical propensity alone is not sufficient for, and does not correlate with, antiviral activity. Inactive peptides with scrambled sequence or amino acid substitutions formed identical CD spectra indicative of α-helix and random coil in TFE and aqueous buffer, respectively.

The anti-HIV activity of peptide HL9 cannot be fully explained by its basicity (pI 12.3) or its secondary structure alone. Other peptides with identical pIs and α-helical structure, such as the HL9 scrambled sequence and the HL9 R→K mutants, do not have anti-HIV activity. Unique amino acid sequence, specific structural features, and folding topologies must be required for anti-HIV activity. Additional studies are necessary to investigate whether HL18 and HL9 are found in vivo, and if they correlate with resistance to viral infection.

HL9 has direct effects on HIV-1 viral entrance as well as replication. There are several potential mechanisms for these effects. As proposed for other cationic peptides (*27*), HL9 may disrupt the viral particle, or prevent its binding and entry into target cells. Alternatively, HL9 may signal the cell in a receptor-dependent manner (*28*) resulting in an intracellular antiviral state that affects a post-entry step(s) in the viral life cycle. The cDNA microarray results on the effect of HL9 on HIV-1 infected target cells provide a sensitive profiling of the host response during viral infection and following antiviral treatment. These findings suggest that the effects of HL9 on signaling pathways involved in survival, stress, TGFβ, p53, NFκB, protein kinase C and hedgehog signaling may reflect changes in host cells that affect susceptibility to infection.

In summary, this is the first identification, structure/activity mapping, and modeling of small anti-HIV mimetics from human lysozyme. HL9 peptide can be easily synthesized and is readily available. The main advantage of host peptides as effectors of innate immunity is that they can function without either high specificity or memory. Structural and functional characterization of natural antimicrobial peptides generated from physiological precursors is of growing interest because of their potential therapeutic applications. We hope that our findings that HL18 and HL9 are active against HIV-1 may lead to new strategies for the treatment of HIV-1 and other viral infections.

REFERENCES

1. Fleming, A. (1922) On a remarkable bacteriolytic element found in tissues and secretions, *Proceedings of the Royal Society Series B 93*, 306−317.
2. Osserman, E. F., Klockars, M., Halper, J., and Fischel, R. E. (1973) Effects of lysozyme on normal and transformed mammalian cells, *Nature 243*, 331−335.
3. Oevermann, A., Engels, M., Thomas, U., and Pellegrini, A. (2003) The antiviral activity of naturally occurring proteins and their peptide fragments after chemical modification, *Antiviral Res 59*, 23−33.
4. Hayashi, M., Okabe, J., and Hozumi, M. (1979) Sensitization of resistant myeloid leukemia clone cells by anti-cancer drugs to factor-stimulating differentiation, *Gann 70*, 235−238.
5. Qi, L., and Ostrand-Rosenberg, S. (2000) MHC class II presentation of endogenous tumor antigen by cellular vaccines depends on the endocytic pathway but not H2-M, *Traffic 1*, 152−160.
6. Siwicki, A. K., Klein, P., Morand, M., Kiczka, W., and Studnicka, M. (1998) Immunostimulatory effects of dimerized lysozyme (KLP-602) on the nonspecific defense mechanisms and protection against furunculosis in salmonids, *Vet Immunol Immunopathol 61*, 369−378.
7. King, A. E., Critchley, H. O., and Kelly, R. W. (2003) Innate immune defences in the human endometrium, *Reprod Biol Endocrinol 1*, 116.
8. Lee-Huang, S., Huang, P. L., Sun, Y., Kung, H. F., Blithe, D. L., and Chen, H. C. (1999) Lysozyme and RNases as anti-HIV components in beta-core preparations of human chorionic gonadotropin, *Proc Natl Acad Sci U S A 96*, 2678−2681.
9. Nara, P. L., and Fischinger, P. J. (1988) Quantitative infectivity assay for HIV-1 and-2, *Nature 332*, 469−470.
10. Lee-Huang, S., Huang, P. L., Nara, P. L., Chen, H. C., Kung, H. F., Huang, P., and Huang, H. I. (1990) MAP 30: a new inhibitor of HIV-1 infection and replication, *FEBS Lett 272*, 12−18.
11. Cory, A. H., Owen, T. C., Barltrop, J. A., and Cory, J. G. (1991) Use of an aqueous soluble tetrazolium/formazan assay for cell growth assays in culture, *Cancer Commun 3*, 207−212.
12. Lee-Huang, S., Zhang, L., Huang, P. L., and Chang, Y. T. (2003) Anti-HIV activity of olive leaf extract (OLE) and modulation of host cell gene expression by HIV-1 infection and OLE treatment, *Biochem Biophys Res Commun 307*, 1029−1037.
13. Shugar, D. (1952) Measurements of lysozyme activity and the ultraviolet inactivation of lysozyme, *Biochim Biophys Acta 8*, 302.
14. Abagyan, R., and Totrov, M. (1994) Biased probability Monte Carlo conformational searches and electrostatic calculations for peptides and proteins, *J Mol Biol 235*, 983−1002.
15. Abagyan, R., and Totrov, M. (1999) Ab initio folding of peptides by the optimal bias Monte Carlo minimization procedure, *J Comp Phys 51*, 402−421.
16. Kabsch, W., and Sander, C. (1983) Dictionary of protein secondary structure: pattern recognition of hydrogen-bonded and geometrical features, *Biopolymers 22*, 2577−2637.
17. Peters, C. W., Kruse, U., Pollwein, R., Grzeschik, K. H., and Sippel, A. E. (1989) The human lysozyme gene. Sequence organization and chromosomal localization, *Eur J Biochem 182*, 507−516.
18. Song, H., Inaka, K., Maenaka, K., and Matsushima, M. (1994) Structural changes of active site cleft and different saccharide binding modes in human lysozyme cocrystallized with hexa-*N*-acetyl-chitohexaose at pH 4.0, *J Mol Biol 244*, 522−540.
19. Maenaka, K., Matsushima, M., Song, H., Sunada, F., Watanabe, K., and Kumagai, I. (1995) Dissection of protein-carbohydrate interactions in mutant hen egg-white lysozyme complexes and their hydrolytic activity, *J Mol Biol 247*, 281−293.
20. Bhatnagar, R. S., and Gough, C. A. (1996) *Circular dichroism and the conformational analysis of biomolecules*, Plenum Press, New York.
21. Miralem, T., Wang, A., Whiteside, C. I., and Templeton, D. M. (1996) Heparin inhibits mitogen-activated protein kinase-dependent and -independent c-fos induction in mesangial cells, *J Biol Chem 271*, 17100−17106.
22. Masschalck, B., and Michiels, C. W. (2003) Antimicrobial properties of lysozyme in relation to foodborne vegetative bacteria, *Crit Rev Microbiol 29*, 191−214.
23. Yoshio, H., Tollin, M., Gudmundsson, G. H., Lagercrantz, H., Jornvall, H., Marchini, G., and Agerberth, B. (2003) Antimicrobial polypeptides of human vernix caseosa and amniotic fluid: implications for newborn innate defense, *Pediatr Res 53*, 211−216.
24. Clare, D. A., Catignani, G. L., and Swaisgood, H. E. (2003) Biodefense properties of milk: the role of antimicrobial proteins and peptides, *Curr Pharm Des 9*, 1239−1255.
25. Pellegrini, A. (2003) Antimicrobial peptides from food proteins, *Curr Pharm Des 9*, 1225−1238.
26. Ibrahim, H. R., Thomas, U., and Pellegrini, A. (2001) A helix-loop-helix peptide at the upper lip of the active site cleft of lysozyme confers potent antimicrobial activity with membrane permeabilization action, *J Biol Chem 276*, 43767−43774.
27. Boman, H. G. (2003) Antibacterial peptides: basic facts and emerging concepts, *J Intern Med 254*, 197−215.
28. Hancock, R. E., and Patrzykat, A. (2002) Clinical development of cationic antimicrobial peptides: from natural to novel antibiotics, *Curr Drug Targets Infect Disord 2*, 79−83.

BI0477081